

On Time-Optimal Trajectories for Differential Drive Vehicles with Field-Of-View Constraints

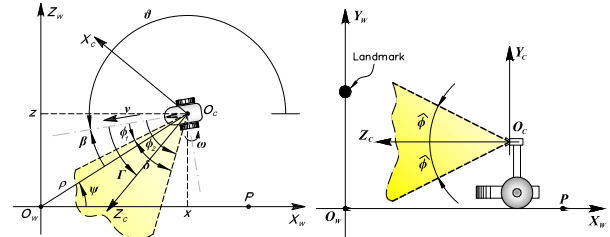
Andrea Cristofaro^{§†}, Paolo Salaris^{*}, Lucia Pallottino^{*}, Fabio Gianni[†], Antonio Bicchi[‡]

Abstract—This paper presents the first step toward the study of minimum time trajectories for a differential drive robot, which is equipped with a fixed and limited Field-Of-View (FOV) camera, towards a desired configuration while keeping a given landmark in sight during maneuvers. While several previous works have provided a complete synthesis of shortest paths in case of both nonholonomic and FOV constraints, to the best of our knowledge, this paper represents the first analysis of minimum time trajectories with the two constraints. After showing the extremals of the problem at hand, i.e. straight lines, rotations on the spot, logarithmic spirals and involute of circles, we provide the optimal control laws that steer the vehicle along the path and the cost in terms of time along each extremal. Moreover, we compare some concatenations of extremals in order to reduce the complexity of the problem toward the definition of a sufficient finite set of optimal maneuvers.

I. INTRODUCTION

Time optimal trajectories for a bounded velocity Differential Drive Robot (DDR) which moves on a unobstructed plane has been derived in [1]. In particular, authors provided a proof of the existence and an analysis of the structure of the time optimal trajectories. Moreover, they furnished an algorithm to determine all optimal trajectories with the associated time. Also in this paper, as in [1], we consider a DDR with bounded velocity but in our case it has a fixed on-board camera with limited Field-Of-View (FOV) – basically further limiting feasible maneuvers. The objective of this research, whereof this paper represents a first attempt, is to derive the time optimal trajectories from any starting configuration of the vehicle to a desired one, while keeping a given landmark in sight during maneuvers. We consider a pinhole camera model ([2]) with a limited horizontal and vertical angle of view (see figure 1) whose principal axis forms and angle Γ w.r.t. the robot forward direction.

Localization tasks and/or maintain visibility of some objects in the environment require that some landmarks must be kept in sight. In visual servoing tasks this problem becomes particularly noticeable and several solutions have been proposed to overcome it. However, when the FOV problem has been successfully solved for nonholonomic vehicle, e.g. in [3], [4], [5], the resultant path is often inefficient and absolutely not optimal. An optimal solution



(a) H-FOV constraints with cartesian and polar coordinates of the robot.

(b) V-FOV constraints.

Fig. 1. Mobile robot and systems coordinates. The robot's task is to reach P while keeping the landmark within a limited FOV (dashed lines).

for a nonholonomic vehicle with FOV constraints has been furnished in [6] and [7]. In particular, [6] provides the shortest paths synthesis in case of a camera modeled as a frontal and symmetric (w.r.t. the forward direction of motion), planar cone, i.e. only horizontal limits of the sensor are taken into account. In [7] shortest paths to generic FOVs, including side and lateral sensors (the forward direction of motion is not included inside the FOV) has been obtained. Moreover, in [8] authors also introduced the vertical constraint limits imposed by the camera.

On the other hand, optimal trajectories for DDRs without FOV constraints are also derived in [9] where the total amount of wheel rotation is optimized, while in [10] time optimal trajectories are obtained for an omnidirectional vehicle. The methodology used in [1] is an extension of optimal control techniques developed in [11], [12], [13] for steered vehicles. Moreover, in [14] a geometric algorithm to derive time optimal trajectories for a bidirectional steered robot is developed. The study of optimal controls for such vehicles started with [15] and [16].

In this paper we start to study time optimal trajectories for a DDR subject to FOV constraints, providing that the extremal maneuvers, i.e. maneuvers that verify the necessary conditions for optimality, are straight lines, rotations on the spot, logarithmic spirals and involutes of circles. We, thus, provide the optimal control laws that steer the vehicle along the extremals and their cost in terms of time along each arc. Finally, we compare some concatenations of extremals in order to obtain a sufficient finite set of time optimal maneuvers.

II. PROBLEM DEFINITION

Consider a differential drive vehicle ([1]) moving on a plane where a right-handed reference frame $\langle W \rangle$ is defined with origin in O_w and axes X_w, Z_w . The configuration of

[†]The research leading to these results has received funding from the European Union Seventh Framework Programme [FP7/2007-2013] under grant agreement n257462 HYCON2 Network of excellence”.

[§] Department of Engineering Cybernetics, NTNU, Trondheim, Norway.

^{*} Interdept. Research Center “Enrico Piaggio”, University of Pisa, Italy.

[†] School of Science and Technology, University of Camerino, 62032 Camerino (MC), Italy.

[‡] Department of Advanced Robotics, Istituto Italiano di Tecnologia, via Morego, 30, 16163 Genova, Italy,

the vehicle is described by $\xi(t) = (x(t), z(t), \theta(t))$, where $(x(t), z(t))$ is the position in $\langle W \rangle$ of a reference point in the vehicle, and $\theta(t)$ is the vehicle heading with respect to the X_w axis (see figure 1). We assume that the dynamics of the vehicle are negligible, and that the forward and angular velocities, $v(t)$ and $\omega(t)$ respectively, are the control inputs of the kinematic model of the vehicle. Choosing polar coordinates (see figure 1), the kinematic model of the unicycle-like robot is

$$\begin{bmatrix} \dot{\rho} \\ \dot{\psi} \\ \dot{\beta} \end{bmatrix} = \begin{bmatrix} -\cos\beta & 0 \\ \frac{\sin\beta}{\rho} & 0 \\ \frac{\sin\beta}{\rho} & -1 \end{bmatrix} \begin{bmatrix} v \\ \omega \end{bmatrix}. \quad (1)$$

Denoting by w_r and w_l the angular velocities of the right and left wheel, respectively, we have

$$v = \frac{w_r + w_l}{2}, \quad \omega = \frac{w_r - w_l}{2b}$$

where b is half of the wheels axle length. We assume $w_i \in [-1, 1]$, $i = r, l$ and the input space is $U = [-1, 1]^2 \subset \mathbb{R}^2$. As a consequence, the forward and angular velocities domain is a convex compact subset $\mathcal{U} \in \mathbb{R}^2$.

The vehicle carries an on-board rigidly fixed pinhole camera with a reference frame $\langle C \rangle = \{O_c, X_c, Y_c, Z_c\}$ such that the optical center O_c corresponds to the robot's center $[x(t), z(t)]^T$ and the optical axis Z_c forms an angle Γ with the robot's forward direction (see figure 1(a)). Without loss of generality, we will assume $0 \leq \Gamma \leq \frac{\pi}{2}$, so that, when $\Gamma = 0$ the Z_c axis is aligned with the robot's forward direction, whereas, when $\Gamma = \frac{\pi}{2}$, the Z_c axis is perpendicular to the robot's forward direction. The camera has a limited Field-Of-View (FOV) whose horizontal and vertical angle of view are δ and ε , respectively. Moreover, let $\hat{\phi}$ be half of the vertical angular aperture, whereas ϕ is half of the horizontal angular aperture. In the following, we consider the most interesting case in which ε and δ are less than $\pi/2$. Consider $\phi_1 = \Gamma - \frac{\delta}{2}$ and $\phi_2 = \Gamma + \frac{\delta}{2}$ the angles between the robot's forward direction and the right and left sensor's border w.r.t. Z_c axis, respectively.

We assume that the feature to be kept within the on-board limited FOV sensor is placed on the axis through the origin O_w , perpendicular to the plane of motion, so that its projection on the motion plane coincides with the center O_w (see figure 1). The feature has height h from the plane $X_c \times Z_c$. Moreover, without loss of generality, let us consider the position of the robot target point P to lay on the X_w axis, with coordinates $(\rho, \psi) = (\rho_P, 0)$.

The horizontal FOV (H-FOV), with characteristic angle $\delta = |\phi_2 - \phi_1|$, generates the following constraints:

$$\beta - \phi_1 \geq 0, \quad (2)$$

$$\beta - \phi_2 \leq 0. \quad (3)$$

while the vertical FOV (V-FOV), with characteristic angle ε , generates the following one

$$\rho \cos(\beta - \Gamma) \geq \frac{h}{\tan \hat{\phi}} := R_b \quad (4)$$

where R_b is a constant and it represents the minimum distance from O_w that the vehicle can reach without violate FOV constraints. Let C_b denote the circumference with radius R_b .

The goal is to determine, for any point $Q \in \mathbb{R}^2$ on the motion plane and orientation of the robot, the minimum time trajectory from Q to P such that the feature in O_w is maintained in the FOV of the sensor. In other words, the problem to be solved is

$$\min_{v, \omega} \int_0^T dt, \quad (5)$$

subject to (1) with controls $(v, \omega) \in \mathcal{U}$ and such that feasibility constraints (2), (3) and (4) are satisfied along the trajectory, i.e. the landmark is always maintained in view.

Remark 1: The H-FOV and the V-FOV constraints (2), (3) and (4) can not be simultaneously active, a part from a 1-dimensional curve C_δ , which is a circumference centered in O_w and with radius $R_\delta = \frac{R_b}{\cos\phi}$. As a consequence, circumferences C_δ and C_b subdivide the motion plane in three zones

$$Z_0 := \{(\rho, \psi) | \rho < R_b\}$$

$$Z_1 := \{(\rho, \psi) | R_b \leq \rho < R_\delta\}$$

$$Z_2 := \{(\rho, \psi) | \rho > R_\delta\}.$$

It is straightforward to show that Z_0 is the inaccessible zone where both V-FOV and H-FOV constraints are violated, Z_1 is the annulus where V-FOV constraint is more restrictive than H-FOV ones and hence in this zone we can only consider the V-FOV constraint (see figure 1(b)). Finally, $Z_2 = \mathbb{R}^2 \setminus (Z_0 \cup Z_1)$ is the zone where H-FOV constraints are more restrictive than V-FOV one, and hence we can assume the camera as a planar cone (see figure 1(a)).

III. OPTIMAL TRAJECTORIES CHARACTERIZATION

In this section we describe the extremal arcs associated to the optimal control problem (5) based on the Pontryagin Minimum Principle. For each arc we also provide the characterization of controls that optimally steer the vehicle along the arc. Finally, the time length of each arc is computed.

A. Adjoint equations and extremal paths

Both H-FOV and V-FOV constraints depend on the states and not (explicitly) on the control variables. In this case the constraints can be derived with respect to the time until the equation depends on the control, see [17]. All the derivatives obtained are introduced in the Hamiltonian function as it is usually done with constraints on the control variables. The constrained Hamiltonian of the system is hence given by

$$\begin{aligned} H(\rho, \psi, \beta, v, \omega) = & 1 - \lambda_1 (\cos\beta)v + \lambda_2 \frac{\sin\beta}{\rho} v \\ & + (\lambda_3 - \mu_1 + \mu_2) \left(\frac{\sin\beta}{\rho} v - \omega \right) \\ & + \mu_3 (-\cos\Gamma v + \rho \sin(\beta - \Gamma)\omega), \end{aligned}$$

with adjoints dynamics $\dot{\lambda}_i = -\frac{\partial H}{\partial \eta_i}$ and $\mu_1, \mu_2, \mu_3 \geq 0$.

1) *Inactive constraints*: Let us suppose that the initial condition $q(0)$ is such that

$$\phi_1 < \beta(0) < \phi_2, \quad \rho(0) \cos(\beta(0) - \Gamma) > R_h,$$

and hence the constraints are not active for an interval $U_1 = [0, t_1[$. From [1], the extremal arcs have been obtained together with the structure of optimal trajectories that consist in at most five extremals. The extremals are rotations on the spot (denoted by $*$) covered at maximum angular velocity and the straight lines (denoted by S) covered at maximum speed. For reader convenience, we explicitly report controls v and ω along such extremals

$$\begin{cases} v = 0 \\ \omega = \pm \frac{1}{b} \end{cases} \quad \text{or} \quad \begin{cases} v = \pm 1 \\ \omega = 0 \end{cases}$$

2) *Active constraints*: Let us assume now that in the interval $[t_1, t_2]$ one of the FOV constraints is active, i.e. one of the conditions (2)-(3) and (4) is verified with the equality sign. For the H-FOV case we have $\beta \equiv \phi_i$ and hence $\tan \beta = \tan \phi_i$. By (1), $\dot{\psi} = \tan \phi_i \frac{\dot{\rho}}{\rho} = \tan \phi_i \frac{d}{dt} (\ln \rho)$. By integration, we obtain the equation of a logarithmic spiral (see [6] for details)

$$\psi = \tan \phi_i \ln \left(\frac{\rho}{\rho_0} \right) + \psi_0, \quad \text{or} \quad \rho = \rho_0 e^{(\psi - \psi_0) \cot \phi_i} \quad (6)$$

where ρ_0 and ψ_0 are constant that depend on initial conditions.

On the other hand, the V-FOV constraint is activated for those configurations that verify

$$\rho \cos(\beta - \Gamma) = R_b. \quad (7)$$

Given (1), the relationship between the control inputs v and ω required to follow a path along which (7) holds is given by

$$\dot{\rho} \cos(\beta - \Gamma) - \rho \sin(\beta - \Gamma) \dot{\beta} = 0 \Rightarrow \rho \sin(\beta - \Gamma) \omega = v \cos \Gamma.$$

From (1), the trajectory followed with such inputs satisfies $\dot{\psi} = -\tan \beta \tan(\beta - \Gamma) \dot{\beta}$ that by integration gives the following relation between ψ and β ,

$$\psi = \psi_b + \beta - \cot \Gamma \log \left(\frac{\cos(\beta - \Gamma)}{\cos \beta} \right) + \cot \Gamma \log(\cos(\Gamma)) \quad (8)$$

For $\Gamma = 0$ the above equation corresponds to an involute of circle with equations:

$$\begin{cases} \rho \cos(\beta) = R_b \\ \psi = \psi_b - \tan \beta + \beta. \end{cases} \quad (9)$$

Paths characterized by equations (9) are curves known as *involute of a circle*¹. On the other hand, equations (7) and (8) correspond to an involute of a circle rotated of an angle Γ around the point (R_b, ψ_b) . With an abuse of notation, in the following, we will refer to this as an involute of circle.

¹The involute of a circle is the path traced out by a point on a straight line r that rolls around a circle without slipping).

To determine how the vehicle covers those arcs along an optimal trajectory, i.e. to choose the optimal values for w_r and w_l , it is necessary to consider the Hamiltonian

$$\bar{H} = 1 + \frac{w_r}{2} s_+ + \frac{w_l}{2} s_- + \frac{w_r}{2} m_+ + \frac{w_l}{2} m_-,$$

where

$$\begin{aligned} s_+ &= \left(-\lambda_1 \cos \beta + \lambda_2 \frac{\sin \beta}{\rho} + \lambda_3 \frac{\sin \beta}{\rho} - \frac{\lambda_3}{b} \right), \quad s_- = s_+ + 2 \frac{\lambda_3}{b}, \\ m_+ &= (\mu_1 - \mu_2) \left(-\frac{\sin \beta}{\rho} + \frac{1}{b} \right) + \mu_3 \left(-\cos \Gamma + \frac{\rho \sin(\beta - \Gamma)}{b} \right), \\ m_- &= m_+ - 2(\mu_1 - \mu_2) \frac{1}{b} - 2\mu_3 \frac{\rho \sin(\beta - \Gamma)}{b}, \end{aligned}$$

with $\mu_1, \mu_2, \mu_3 \geq 0$. From Remark 1, one has necessarily $\mu_1 \mu_2 = 0$ and $(\mu_1 + \mu_2) \mu_3 = 0$, that is the three constraints cannot be active simultaneously so as the two horizontal constraints. Hence we now consider the conditions on the derivatives of the constraints activated in $[t_1, t_2]$, as function of w_r, w_l , for the H-FOV and the V-FOV cases separately.

For the H-FOV constraints we have

$$\dot{\beta} = \frac{\sin \beta (w_r + w_l)}{2\rho} - \frac{w_r - w_l}{2b} = 0. \quad (10)$$

Hence for $\beta = \Gamma \pm \frac{\delta}{2} = \phi_i$ $i = 1, 2$, from (10), the two wheels velocities must satisfy

$$w_r (\rho - b \sin \phi_i) = w_l (\rho + b \sin \phi_i). \quad (11)$$

The Hamiltonian, with $\mu_3 = 0$, can be rewritten as

$$H = 1 + w_r \left(\lambda_2 \frac{\sin \phi_i}{\rho} - \lambda_1 \cos \phi_i \right) \frac{\rho}{b \sin \phi_i + \rho} =: 1 + w_r r_+ \quad (12)$$

or equivalently

$$H = 1 + w_l \left(\lambda_2 \frac{-\sin \phi_i}{\rho} + \lambda_1 \cos \phi_i \right) \frac{\rho}{b \sin \phi_i - \rho} =: 1 + w_l r_- \quad (13)$$

If $\sin \phi_i \geq 0$ then the Hamiltonian is minimized selecting $w_r = -\text{sign } r_+$ in (12). Indeed, in this case, $|w_r| = 1$ and, from (11), $|w_l| < 1$. Similarly, if $\sin \phi_i < 0$ we have $w_l = -\text{sign } r_-$ in (13). In this case $|w_l| = 1$ and, from (11), $|w_r| < 1$. Hence, constraint $(w_r, w_l) \in [-1, 1]^2$ is fulfilled. From results in [6], [7] we know that condition (10) corresponds to a spiral arc. Hence, the spiral is followed by the vehicle with the outer wheel has maximum angular velocity while the inner one follows according to (11).

From the results obtained in [8] we know that the V-FOV constraints corresponds to an involute of circle. For space limitations and for the sake of simplicity, we consider the case $\Gamma = 0$. Consider the equation of the involute given by $\psi = \tan \beta - \beta + \psi_0$ (see [8]) we have

$$\begin{aligned} \frac{d}{dt} [\psi - \tan \beta + \beta - \psi_0] &= \\ (2 + \tan^2 \beta) \frac{w_r - w_l}{2b} - \frac{\sin \beta}{\rho} (1 + \tan^2 \beta) \frac{w_r + w_l}{2} &= 0 \end{aligned} \quad (14)$$

From (14), the wheels velocities must satisfy the following relation:

$$w_r \left(3 + \cos(2\beta) - 2b \frac{\sin \beta}{\rho} \right) = w_l \left(3 + \cos(2\beta) + 2b \frac{\sin \beta}{\rho} \right). \quad (15)$$

Considering $\mu_1 = \mu_2 = 0$, also in this case, the Hamiltonian can be rewritten in the form

$$H = 1 + w_r t_+ \quad (16)$$

$$H = 1 + w_l t_- \quad (17)$$

If $\beta \in [0, \pi/2]$ we have $\sin\beta \geq 0$ then the Hamiltonian is minimized selecting $w_r = -\text{sign } t_+$ in (16). Indeed, in this case, $|w_r| = 1$ and, from (15), $|w_l| < 1$. Similarly, if $\beta \in [-\pi/2, 0]$ we have $\sin\beta \leq 0$ we have $w_l = -\text{sign } t_-$ in (17). In this case $|w_l| = 1$ and, from (15), $|w_r| < 1$. Hence, constraint $(w_r, w_l) \in [-1, 1]^2$ is fulfilled. Hence, the involute is followed by the vehicle with the outter wheel has maximum angular velocity while the inner one follows according to (15).

In conclusion we have four possible type of extremal paths: rotations on the spot $*$, straight lines S , logarithmic spirals T and involutes of a circle I . Notice that both the two H-FOV constraints lead to two logarithmic spirals with two characteristic angles ϕ_1 and ϕ_2 denoted by T_1 and T_2 respectively. The same apply to the V-FOV constraint that lead to two involute of circles evolving clockwise and counterclockwise denoted by I^R and I^L , respectively.

Proposition 3.1: Optimal trajectories are concatenations of extremal paths E , with $E \in \mathcal{E} = \{*, S, T_1, T_2, I^R, I^L\}$.

We recall that we use a superscript sign over the arcs to denote the sign of the linear velocity used to cover the arc. For example, symbols T_1^+ and T_2^- denote an arc of logarithmic spiral with characteristic angle ϕ_1 covered forward and backward, respectively.

The proof of the existence of the optimal trajectory and the proof that it consists in a finite number of switches among extremal arcs are quite long and technical and for space limitations could not be included in this paper². On the other hand, it is important to determine the finite set of extremal sequences that characterize the optimal trajectories and a first step in this direction is done in the rest of the paper.

B. Extremals Time costs

Given a path γ from Q_1 to Q_2 , we denote by $\mathcal{T}^*(\gamma, \beta_{Q_1}, \beta_{Q_2})$ the time cost associated to γ with prescribed initial and final orientations β_{Q_1}, β_{Q_2} . We, thus, denote by $\mathcal{T}(\gamma) = \min_{\beta_{Q_1}, \beta_{Q_2}} \mathcal{T}^*(\gamma, \beta_{Q_1}, \beta_{Q_2})$. By definition one has in general

$$\mathcal{T}^*(\gamma, \beta_{Q_1}, \beta_{Q_2}) \geq \mathcal{T}(\gamma).$$

Let us compute the time costs associated to extremal paths $E \in \mathcal{E}$. Recalling that $|\mathbf{v}| \leq 1$ and $|\omega| \leq 1/b$, the case of extremal paths with inactive constraints is trivial.

Proposition 3.2: The time cost of a straight line from Q_1 to Q_2 , say $S_{Q_1 Q_2}$, is equal to the distance between the two points:

$$\mathcal{T}(S_{Q_1 Q_2}) = \text{dist}(Q_1, Q_2) = \overline{Q_1 Q_2}.$$

Proposition 3.3: The time cost of a rotation on the spot of an angle β , say $*_\beta$, is given by

$$\mathcal{T}(*_\beta) = b|\beta|.$$

In order to evaluate the time cost of spirals and involutes, the following simple formula with $f = \rho$ or $f = \beta$ will be helpful:

$$t = \int_0^t \frac{\dot{f}(s)}{\dot{f}(s)} ds = \int_{f(0)}^{f(t)} \frac{df}{\dot{f}(f)}, \quad \dot{f} \neq 0. \quad (18)$$

Proposition 3.4: Given an arc of logarithmic spiral $T_{Q_1 Q_2}$ from $Q_1 = (\rho_{Q_1}, \psi_{Q_1})$ to $Q_2 = (\rho_{Q_2}, \psi_{Q_2})$, the time cost is

$$\mathcal{T}(T_{Q_1 Q_2}) = \frac{|\rho_{Q_1} - \rho_{Q_2}|}{\cos \phi_i} + b|\psi_{Q_1} - \psi_{Q_2}|, \quad i = 1, 2.$$

Proof: For the sake of simplicity, let us assume $\beta = \phi_1$ with $\sin(\phi_1) > 0$ and $\rho_{Q_1} < \rho_{Q_2}$ along the path $\gamma = T_{Q_1 Q_2}$. From (11) and from the necessary conditions of optimality for w_r and w_l , on this path the vehicle is driven by the velocity $\mathbf{v} = -\frac{\rho}{\rho + b \sin \phi_1}$. The case $\beta = \phi_2$ can be treated in a similar way.

From (18) with $f = \rho$, one has

$$\begin{aligned} \mathcal{T}(T_{Q_1 Q_2}) &= \int_{\rho_{Q_1}}^{\rho_{Q_2}} \frac{d\rho}{-\cos \phi_1 \mathbf{v}} = \int_{\rho_{Q_1}}^{\rho_{Q_2}} \left(\frac{1}{\cos \phi_1} + \frac{b \tan \phi_1}{\rho} \right) d\rho \\ &= \frac{\rho_{Q_2} - \rho_{Q_1}}{\cos \phi_1} + b \tan \phi_1 \log \left(\frac{\rho_{Q_2}}{\rho_{Q_1}} \right). \end{aligned}$$

The conclusion follows from the equation of spirals in (6). \blacksquare

The time $\mathcal{T}(T_{Q_1 Q_2})$ is hence given by the sum of the length fo the spiral between Q_1 and Q_2 and the time equivalent to a rotation on the spot of an angle $|\psi_{Q_1} - \psi_{Q_2}|$.

Proposition 3.5: Given an arc of involute $I_{Q_1 Q_2}$ from $Q_1 = (\rho_{Q_1}, \psi_{Q_1})$ to $Q_2 = (\rho_{Q_2}, \psi_{Q_2})$, the time cost is

$$\begin{aligned} \mathcal{T}(I_{Q_1 Q_2}) &= R_b(\zeta_v(\beta_{Q_2}, \Gamma) - \zeta_v(\beta_{Q_1}, \Gamma)) \\ &\quad + b(\zeta_\omega(\beta_{Q_2}, \Gamma) - \zeta_\omega(\beta_{Q_1}, \Gamma)), \end{aligned}$$

where $\beta_{Q_i} = \arccos(R_b/\rho_{Q_i}) + \Gamma$, $i = 1, 2$ and

$$\zeta_v(\beta, \Gamma) = \left(\frac{\cot \Gamma}{\sin \Gamma} \log \left(\frac{\cos(\beta - \Gamma)}{\cos \beta} \right) - \frac{2 \sin \beta}{\sin 2\Gamma \cos(\beta - \Gamma)} \right)$$

$$\zeta_\omega(\beta, \Gamma) = \cot \Gamma \left(\log \left(\frac{\cos(\beta - \Gamma)}{\cos \beta} \right) \right).$$

Proof: Thanks to the symmetry of the problem, without loss of generality we consider the right involute (I^R) starting from the point $(R_b, 0)$. Such curve can be parametrized as

$$\begin{cases} x(s) = R_b(\cos s + s \sin s) \\ y(s) = R_b(-\sin s + s \cos s) \\ s = \pm \sqrt{\frac{1}{\cos^2(\beta - \Gamma)} - 1} = \pm \tan(\beta - \Gamma), \quad \beta \in [\Gamma, \pi/2 + \Gamma]. \end{cases}$$

Let us also assume that the vehicle starting from point $(R_b, 0)$ moves backward along I^R . From optimality considtions we have that $w_r = -1$ and hence, the optimal linear and angular velocities of the vehicle along this curve are given by $\mathbf{v} = -\frac{\rho \sin(\beta - \Gamma)}{\rho \sin(\beta - \Gamma) + b \cos \Gamma}$, $\omega = -\frac{\cos \Gamma}{\rho \sin(\beta - \Gamma) + b \cos \Gamma}$ and hence, by using (18) with $f = \beta$ and that $\rho \cos(\beta - \Gamma) = R_b$ along an involute,

²The proofs can be found at http://www.centropiaggio.unipi.it/sites/default/files/HVFOV_timeopt.pdf

we obtain

$$\begin{aligned}
\mathcal{T}(I_{Q_1 Q_2}) &= \int_{\beta_{Q_1}}^{\beta_{Q_2}} \frac{\rho d\beta}{\sin \beta v - \omega \rho} = \\
&= R_b \left(\frac{\cot \Gamma}{\sin \Gamma} \log \left(\frac{\cos(\beta - \Gamma)}{\cos \beta} \right) - \frac{2 \sin \beta}{\sin 2\Gamma \cos(\beta - \Gamma)} \right) \Big|_{\beta_{Q_1}}^{\beta_{Q_2}} \\
&\quad + b \cot \Gamma \left(\log \left(\frac{\cos(\beta - \Gamma)}{\cos \beta} \right) \right) \Big|_{\beta_{Q_1}}^{\beta_{Q_2}} = \\
&= R_b \zeta_v(\beta, \Gamma) \Big|_{\beta_{Q_1}}^{\beta_{Q_2}} + b \zeta_\omega(\beta, \Gamma) \Big|_{\beta_{Q_1}}^{\beta_{Q_2}}
\end{aligned}$$

Remark 3.1: In the symmetric case $\Gamma = 0$ the expression of the time cost $\mathcal{T}(I_{Q_1 Q_2})$ can be substantially simplified observing that

$$\lim_{\Gamma \rightarrow 0} \zeta_v(\beta, \Gamma) = \frac{1}{2} (\tan^2 \beta - 1), \quad \lim_{\Gamma \rightarrow 0} \zeta_\omega(\beta, \Gamma) = \tan \beta.$$

In particular for $\Gamma = 0$ one has

$$\begin{aligned}
\mathcal{T}(I_{Q_1 Q_2}) &= \frac{R_b}{2} (\tan^2 \beta_{Q_2} - \tan^2 \beta_{Q_1}) + b(\tan \beta_{Q_2} - \tan \beta_{Q_1}) \\
&= \frac{R_b}{2} \left(\frac{1}{\cos^2 \beta_{Q_2}} - \frac{1}{\cos^2 \beta_{Q_1}} \right) + b(\tan \beta_{Q_2} - \tan \beta_{Q_1}).
\end{aligned}$$

The time $\mathcal{T}(I_{Q_1 Q_2})$ is hence given by the sum of the length of the involute between Q_1 and Q_2 and the time equivalent to a rotation on the spot of an angle $|\tan \beta_{Q_1} - \tan \beta_{Q_2}|$.

IV. OPTIMAL CONCATENATIONS

This section is devoted to the study of optimal concatenations of extremal paths. Indeed, the final goal of this study is to characterize the concatenations that do not belong to optimal path under given conditions on the initial and final configurations.

For space limitations and for the sake of clarity we assume $\Gamma = 0$. In this case $-\phi_1 = \phi_2 = \phi \geq 0$ and the arcs of spiral are denoted by $T_1 = T^R$ and $T_2 = T^L$ similarly to the involutes notation. Referring to Fig. 2, we consider three distinct cases:

- Case 1: comparison between $T^+ * T^-$ and $T^- * T^+$
- Case 2: comparison between $I^+ * I^-$ and $I^- * I^+$
- Case 3: comparison between $T^+ * T^-$ and $I^- * I^+$

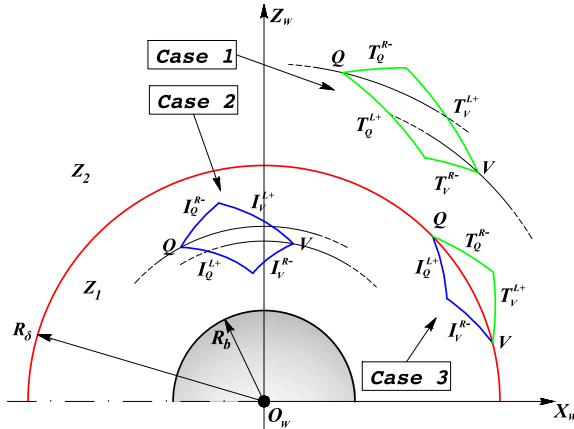


Fig. 2. Pairs of spirals and involutes arcs for length comparison

A. Case 1: Comparison between pairs of spiral arcs

Let us consider two points $Q = (\rho_Q, \psi_Q)$ and $V = (\rho_V, \psi_V)$ with $\psi_Q \geq \psi_V$, $\rho_Q \geq \rho_V$. There are two possible pairs of spirals from Q to V : $\gamma_1 = T_Q^{L+} * T_V^{R-}$ and $\gamma_2 = T_Q^{R-} * T_V^{L+}$. The equations of the curves are

$$\begin{aligned}
T_Q^{L+}: \quad \rho(\psi) &= \rho_Q e^{(\psi - \psi_Q) \cot \phi} \\
T_V^{R-}: \quad \rho(\psi) &= \rho_V e^{-(\psi - \psi_V) \cot \phi}
\end{aligned}$$

$$\begin{aligned}
T_V^{R-}: \quad \rho(\psi) &= \rho_Q e^{-(\psi - \psi_Q) \cot \phi} \\
T_Q^{L+}: \quad \rho(\psi) &= \rho_V e^{(\psi - \psi_V) \cot \phi}
\end{aligned}$$

and therefore the corresponding intersection points, between the two spirals of the paths, $\hat{H}_1 = (\hat{\rho}_{\gamma_1}, \hat{\psi}_{\gamma_1})$ and $\hat{H}_2 = (\hat{\rho}_{\gamma_2}, \hat{\psi}_{\gamma_2})$ are given by

$$\begin{aligned}
\hat{\rho}_{\gamma_1} &= \sqrt{\rho_Q \rho_V} e^{\frac{\psi_V - \psi_Q}{2} \cot \phi}, \quad \hat{\psi}_{\gamma_1} = \frac{\log \rho_V - \log \rho_Q}{2 \cot \phi} + \frac{\psi_Q + \psi_V}{2}, \\
\hat{\rho}_{\gamma_2} &= \sqrt{\rho_Q \rho_V} e^{\frac{\psi_Q - \psi_V}{2} \cot \phi}, \quad \hat{\psi}_{\gamma_2} = \frac{\log \rho_Q - \log \rho_V}{2 \cot \phi} + \frac{\psi_Q + \psi_V}{2},
\end{aligned}$$

with

$$\begin{cases} \psi_V \leq \hat{\psi}_{\gamma_1} \leq \psi_Q, & \psi_V \leq \hat{\psi}_{\gamma_2} \leq \psi_Q, \\ \hat{\rho}_{\gamma_1} \leq \rho_V \leq \rho_Q \leq \hat{\rho}_{\gamma_2}, \end{cases} \quad (19)$$

Such spirals can be compared only if γ_1 lays in Z_2 , i.e. $\hat{\rho}_{\gamma_1} > R_d$.

Proposition 1: Given Q and V and the path γ_1 and γ_2 defined above, it holds:

$$\mathcal{T}(\gamma_2) = \mathcal{T}_2 \geq \mathcal{T}(\gamma_1) = \mathcal{T}_1.$$

To prove this proposition we need the following:

Lemma 4.1: Given $x, y, z \in (0, \infty)$ with $x \geq y$ and $z \geq 1$, the following conditions are equivalent

- $x \leq z\sqrt{xy}$,
- $y \geq \frac{\sqrt{xy}}{z}$,
- $\sqrt{xy}(z + 1/z) \geq x + y$.

Proof: The equivalence between i) and ii) follows immediately observing that

$$y \geq \frac{\sqrt{xy}}{z} \Leftrightarrow \frac{1}{y} \leq \frac{z}{\sqrt{xy}} \Leftrightarrow \sqrt{\frac{x}{y}} \leq z \Leftrightarrow x \leq z\sqrt{xy}.$$

On the other hand condition iii) can be rewritten as

$$\frac{(z^2 + 1)\sqrt{xy} - z(x + y)}{z\sqrt{xy}} \geq 0,$$

whose solutions $z \geq 1$ satisfy

$$z \geq \frac{(x + y) + (x - y)}{2\sqrt{xy}} = \sqrt{\frac{x}{y}}.$$

We can now prove the Proposition 1.

Proof: The minimum time to cover the paths γ_1 and γ_2 is given by

$$\begin{aligned}
\mathcal{T}_{\gamma_1} &= \frac{\rho_Q - \hat{\rho}_{\gamma_1}}{\cos \phi} + b(\psi_Q - \hat{\psi}_{\gamma_1}) + \frac{\rho_V - \hat{\rho}_{\gamma_1}}{\cos \phi} + b(\hat{\psi}_{\gamma_1} - \psi_V) + 2b\phi \\
&= \frac{\rho_Q + \rho_V - 2\hat{\rho}_{\gamma_1}}{\cos \phi} + b(\rho_Q - \rho_V) + 2b\phi,
\end{aligned}$$

$$\begin{aligned}
\mathcal{T}_{\gamma_2} &= \frac{\hat{\rho}_{\gamma_2} - \rho_Q}{\cos \phi} + b(\psi_Q - \hat{\psi}_{\gamma_2}) + \frac{\hat{\rho}_{\gamma_2} - \rho_V}{\cos \phi} + b(\hat{\psi}_{\gamma_2} - \psi_V) + 2b\phi \\
&= \frac{2\hat{\rho}_{\gamma_2} - (\rho_Q + \rho_V)}{\cos \phi} + b(\rho_Q - \rho_V) + 2b\phi.
\end{aligned}$$

By subtraction one gets

$$\mathcal{T}_{\gamma_2} - \mathcal{T}_{\gamma_1} = \frac{2}{\cos\phi} (\hat{\rho}_{\gamma_1} + \hat{\rho}_{\gamma_2} - \rho_Q - \rho_V).$$

The conclusion $\mathcal{T}_{\gamma_2} - \mathcal{T}_{\gamma_1} \geq 0$ is equivalent to $\hat{\rho}_{\gamma_1} + \hat{\rho}_{\gamma_2} \geq \rho_Q + \rho_V$ that follows from Lemma 4.1 with $x = \rho_Q$, $y = \rho_V$ and $z = e^{\frac{\psi_Q - \psi_V}{2} \cot\phi}$. Indeed, the condition $\rho_Q \leq \rho_{\gamma_2}$, in (19), is $x \leq z\sqrt{xy}$. From Lemma 4.1, this is equivalent to $\sqrt{xy}(z+1/z) \geq x+y$ and hence the thesis. ■

B. Case 2: Comparison between pairs of involutes

Consider two points Q and V with $\rho_Q = \rho_V$ we set $\beta_Q = -\beta_Q = \arccos \frac{R_b}{\rho_Q}$. From the equation of involutes (9), ψ_Q and ψ_V are obtained and $|\psi_Q - \psi_V| = \widehat{QO_WV} = \Delta\psi > 0$;

Consider the two possible concatenations of involute curves from Q to V :

$$\mathcal{C}_1 = I_Q^+ * I_V^-, \quad \mathcal{C}_2 = I_Q^- * I_V^+.$$

Those curves can be compared only if \mathcal{C}_2 lays inside Z_1 . As proved in [8], denoting by $\ell(\gamma)$ the length of the path γ , there exists $\bar{\rho} > \sqrt{2}R_b$ such that

$$\begin{cases} \ell(\mathcal{C}_1) \leq \ell(\mathcal{C}_2) & \rho_Q \geq \bar{\rho}, \\ \ell(\mathcal{C}_2) \leq \ell(\mathcal{C}_1) & \rho_Q \leq \sqrt{2}R_b. \end{cases}$$

On the other hand the following identities are straightforward to check for an arbitrary involute arc I from Q to V and curves $\mathcal{C}_1, \mathcal{C}_2$:

$$\begin{aligned} \mathcal{T}(I) &= \ell(I) + b|\tan\beta_V - \tan\beta_Q| \\ \mathcal{T}(\mathcal{C}_1) &= \ell(\mathcal{C}_1) + 2b(\tan\beta_Q - \tan\beta_{H_1}) + 2b\beta_{H_1} \\ \mathcal{T}(\mathcal{C}_2) &= \ell(\mathcal{C}_2) + 2b(\tan\beta_{H_2} - \tan\beta_Q) + 2b\beta_{H_2}, \end{aligned}$$

where we have denoted by H_i the switching point between the involutes in the \mathcal{C}_i curve, $i = 1, 2$. As a consequence, since by construction $\beta_{H_1} < \beta_{H_2}$, one can infer that

$$\mathcal{T}(\mathcal{C}_1) \leq \mathcal{T}(\mathcal{C}_2) \text{ for } \rho_Q \geq \bar{\rho}.$$

The converse case $\rho_Q \leq \bar{\rho}$ leads to different scenarios, depending on several parameters: the radius ρ_Q itself, the angle $\Delta\psi$ and the weight parameter b . We will highlight this fact through some illustrative examples. Prior to present the numerical tests, we introduce a helpful result.

Example 1: Let us consider $\rho_Q = \sqrt{2}R_b$ with $R_b = 1$, that is $\beta_Q = \pi/4$. Fig. 3 illustrates the behavior of $\mathcal{T}(\mathcal{C}_1) - \mathcal{T}(\mathcal{C}_2)$ for different values of b as $\Delta\psi$ varies in $[0, 2\bar{\beta}]$, with $\tan\bar{\beta} - \beta = \pi/4$, i.e. $\bar{\beta} \in [0, \pi/4]$. Notice that, small values of $\bar{\beta}$ correspond to small values of $\Delta\psi$ and viceversa. It can be easily observed that, as b increases, the measure of the interval of positivity of $\mathcal{T}(\mathcal{C}_1) - \mathcal{T}(\mathcal{C}_2)$ decreases. In particular, there exist values of b such that \mathcal{C}_1 is shorter in time with respect to \mathcal{C}_2 . On the other hand, in general, for small amplitude of spanned angles, i.e. small values of $\bar{\beta}$, along the circumference of radius $\sqrt{2}R_b$ the fastest path is \mathcal{C}_2 while for large amplitude of spanned angles, i.e. large values of $\bar{\beta}$, the fastest path is \mathcal{C}_1 . Hence, the fastest path depends on the initial and final configurations.

Example 2: In this second example we would like to illustrate the behavior of $\mathcal{T}(\mathcal{C}_1) - \mathcal{T}(\mathcal{C}_2)$ as β_Q varies. To

this end, let us consider $b = 0.08$ and evaluate the time-costs for different values of β_Q as $\Delta\psi$ varies in $[0, 2\bar{\beta}]$ where $\tan\bar{\beta} - \beta = \pi/6$. Notice that, as expected, for small values of $\Delta\psi$ the fastest path is \mathcal{C}_2 while for large values of $\Delta\psi$ the fastest path is \mathcal{C}_1 (see Fig. 4).

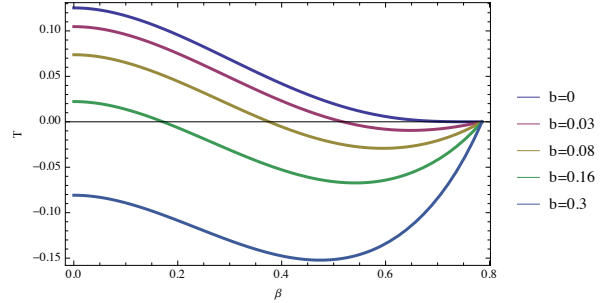


Fig. 3. Evaluation of $\mathcal{T}(\mathcal{C}_1) - \mathcal{T}(\mathcal{C}_2)$ with $\beta_Q = \pi/4$ for different values of the parameter b .

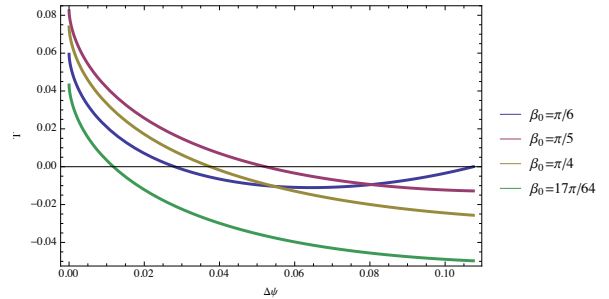


Fig. 4. Evaluation of $\mathcal{T}(\mathcal{C}_1) - \mathcal{T}(\mathcal{C}_2)$ with $b = 0.08$ for different values of the heading angle β_Q .

C. Case 3: Comparing pairs of spirals with pairs of involutes

We are now able to consider the cases in which one of the spiral pairs or the involute pairs intersect Z_1 or Z_2 , respectively. We hence consider two points Q and V on the circumference $C_\delta = Z_1 \cap Z_2$, refer to Remark 1, such that $\widehat{QO_WV} = \Delta\psi$. Let us consider the pair of spirals $\gamma_1 = T_Q^- * T_V^+$ with switching point H_1 and the pair of involutes $\mathcal{C}_2 = I_Q^+ * I_V^-$ with switching point H_2 such that $\Delta\psi = 2(\tan(\delta/2) - \delta/2 - \tan(\beta_{H_2}) + \beta_{H_2})$. The time costs of the two concatenations are given by the following formulae:

$$\begin{aligned} \mathcal{T}(\gamma_1) &= \frac{2R_h(e^{\frac{\Delta\psi}{2} \cot \frac{\delta}{2}} - 1)}{\cos^2 \frac{\delta}{2}} + b\Delta\psi + b\delta \\ \mathcal{T}(\mathcal{C}_2) &= R_h \left(\frac{1}{\cos^2 \frac{\delta}{2}} - \frac{1}{\cos^2 \beta_{H_2}} \right) \\ &\quad + 2b(\tan \frac{\delta}{2} - \tan \beta_{H_2}) + 2b\beta_{H_2}. \end{aligned}$$

Proposition 4.1: The difference $\mathcal{T}(\gamma_1) - \mathcal{T}(\mathcal{C}_2)$ does not depend on the parameter b , i.e.

$$\mathcal{T}(\gamma_1) - \mathcal{T}(\mathcal{C}_2) = \ell(\gamma_1) - \ell(\mathcal{C}_2).$$

Proof: In order to prove the statement it is sufficient to observe that $\tan \frac{\delta}{2} - \tan \beta_{H_2} + \beta_{H_2} = \frac{\Delta\psi}{2} + \frac{\delta}{2}$. ■ Due to the proposition above, the behavior of the concatenations is completely determined by the length of the paths; to

this purpose, in the next result we state a necessary condition for the ordering of $\ell(\gamma_1)$ and $\ell(\mathcal{C}_2)$.

Lemma 4.2: The following condition holds true:

$$\ell(\gamma_1) > \ell(\mathcal{C}_2) \quad \text{if } \Delta\psi > 2 \log \frac{3}{2} \tan \frac{\delta}{2} =: \tilde{\delta}$$

Proof: For space limitations we can not report here the length of the paths γ_1 and \mathcal{C}_2 that can be computed by the equations of $2\mathcal{T}(T_{Q,H_1})$ and of $2\mathcal{T}(I_{Q,H_2})$ with $b = 0$. Indeed, imposing $b = 0$ the minimum time corresponds to a minimum length. A sketch of the proof follows. The statement can be verified observing that

$$\ell(\gamma_1) - \ell(\mathcal{C}_2) = \frac{2e^{\frac{\Delta\psi}{2} \cot \frac{\delta}{2}} - 3}{\cos^2 \frac{\delta}{2}} + \frac{1}{\cos^2 \beta_{H_2}}$$

and hence $2e^{\frac{\Delta\psi}{2} \cot \frac{\delta}{2}} > 3 \Rightarrow \ell(\gamma_1) > \ell(\mathcal{C}_2)$. ■

In order to illustrate the converse case $\Delta\psi < \tilde{\delta}$, we present the following examples.

Example 3: Setting $R_h = 1$, the difference $\ell(\gamma_1) - \ell(\mathcal{C}_2)$ has been evaluated as β varies in $[0, \delta/2]$, that is $\Delta\psi \in [0, 2 \tan(\delta/2) - \delta]$, for different values of $\delta/2$. Referring to Fig. 5, it can be noticed that, if $\delta/2 \leq \pi/5$, the inequality $\ell(\mathcal{C}_2) \geq \ell(\gamma_1)$ holds true for any $\beta \in [0, \delta/2]$; conversely, if $\delta/2 > \pi/5$ then $\ell(\mathcal{C}_2) < \ell(\gamma_1)$ for large values of β .

Example 4: Setting again $R_h = 1$, the difference $\ell(\gamma_1) - \ell(\mathcal{C}_2)$ has been evaluated as $\delta/2$ varies in $[\pi/8, \pi/2]$ for different values of $\Delta\psi$. As clearly shown in Fig. 6, all depicted curves share the same behavior: for any given $\Delta\psi$, the curve \mathcal{C}_2 is faster than γ_1 for small values of $\delta/2$.

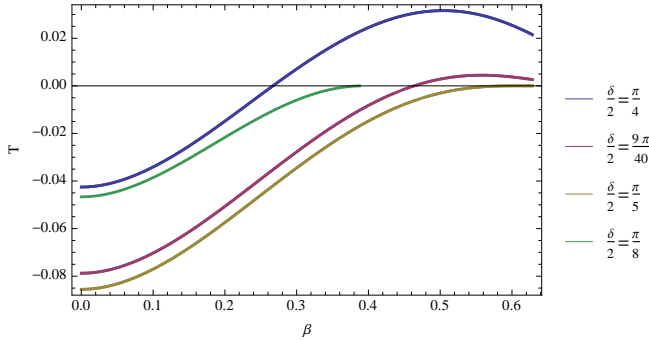


Fig. 5. Evaluation of $\mathcal{T}(\gamma_1) - \mathcal{T}(\mathcal{C}_2)$ for different values of the angle $\delta/2$.

V. CONCLUSION AND FUTURE WORKS

In this paper we have approached the study of minimum time trajectories for a differential drive robot, which is equipped with a fixed and limited Field-Of-View (FOV) camera, towards a desired configuration while keeping a given landmark in sight during maneuvers. We have started comparing some concatenations of extremals in order to reduce the complexity of the problem toward the definition of a sufficient finite set of optimal maneuvers.

Still some work must be done to conclude the analysis of optimal trajectory in order to exclude other concatenations. For example, concatenations of involutes or spiral with straight arc should be considered. Moreover, the time optimal synthesis with feedback control law is also under investigation.

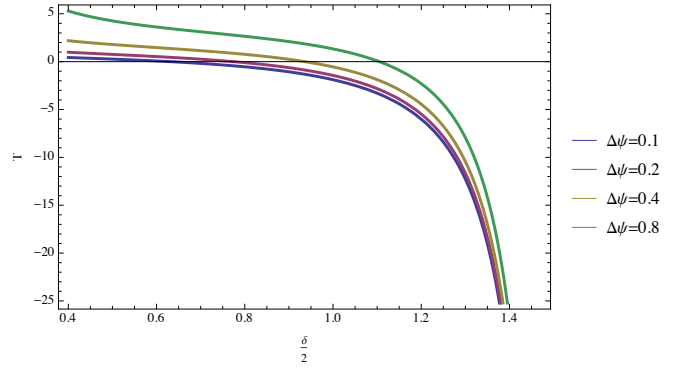


Fig. 6. Evaluation of $\mathcal{T}(\gamma_1) - \mathcal{T}(\mathcal{C}_2)$ for different values of the spanned angle $\Delta\psi$.

REFERENCES

- [1] D. J. Balkcom and M. T. Mason, "Time optimal trajectories for bounded velocity differential drive vehicles," *The International Journal of Robotics Research*, vol. 21, no. 3, pp. 199–217, 2002.
- [2] R. Hartley and A. Zisserman, *Multiple View Geometry in Computer Vision*. Cambridge University Press, 2003.
- [3] P. Murrieri, D. Fontanelli, and A. Bicchi, "A hybrid-control approach to the parking problem of a wheeled vehicle using limited view-angle visual feedback," *Int. Jour. of Robotics Research*, vol. 23, no. 4–5, pp. 437–448, April–May 2004.
- [4] N. Gans and S. Hutchinson, "Stable visual servoing through hybrid switched system control," *IEEE Transactions on Robotics*, vol. 23, no. 3, pp. 530–540, June 2007.
- [5] —, "A stable vision-based control scheme for nonholonomic vehicles to keep a landmark in the field of view," in *Proc. IEEE Int. Conf. on Robotics and Automation*, Apr. 2007, pp. 2196–2201.
- [6] P. Salaris, D. Fontanelli, L. Pallottino, and A. Bicchi, "Shortest paths for a robot with nonholonomic and field-of-view constraints," *IEEE Transactions on Robotics*, vol. 26, no. 2, pp. 269–281, April 2010.
- [7] P. Salaris, L. Pallottino, and A. Bicchi, "Shortest paths for finned, winged, legged, and wheeled vehicles with side-looking sensors," *The International Journal of Robotics Research*, vol. 31, no. 8, pp. 997–1017, 2012.
- [8] P. Salaris, A. Cristofaro, L. Pallottino, and A. Bicchi, "Shortest paths for wheeled robots with limited field-of-view: introducing the vertical constraint," in *Decision and Control, 2013 CDC 2013. Proceedings of the 52th IEEE Conference on*, 2013, pp. 5143–5149.
- [9] H. Chitsaz, S. M. LaValle, D. J. Balkcom, and M. Mason, "Minimum wheel-rotation for differential-drive mobile robots," *The International Journal of Robotics Research*, pp. 66–80, 2009.
- [10] D. Balkcom and M. Mason, "Time-optimal trajectories for an omnidirectional vehicle," *The International Journal of Robotics Research*, vol. 25, no. 10, pp. 985–999, 2006.
- [11] H. Sussmann and G. Tang, "Shortest paths for the reeds-shepp car: A worked out example of the use of geometric techniques in nonlinear optimal control," Department of Mathematics, Rutgers University, Tech. Rep., 1991.
- [12] H. Souères and J. P. Laumond, "Shortest paths synthesis for a car-like robot," *IEEE Transaction on Automatic Control*, pp. 672–688, 1996.
- [13] P. Souères and J. D. Boissonnat, *Optimal Trajectories for Nonholonomic Mobile Robots*. H. Souères and J. P. Laumond: Lecture note in control and information science, 1998, vol. 229.
- [14] H. Wang, Y. Chen, and P. Soueres, "A geometric algorithm to compute time-optimal trajectories for a bidirectional steered robot," *Robotics, IEEE Transactions on*, vol. 25, no. 2, pp. 399–413, April 2009.
- [15] L. E. Dubins, "On curves of minimal length with a constraint on average curvature, and with prescribed initial and terminal positions and tangents," *American Journal of Mathematics*, pp. 457–516, 1957.
- [16] J. A. Reeds and L. A. Shepp, "Optimal paths for a car that goes both forwards and backwards," *Pacific Journal of Mathematics*, pp. 367–393, 1990.
- [17] A. Bryson and Y. Ho, *Applied optimal control*. Wiley New York, 1975.